The impact of standard semiconductor fabrication processes on polycrystalline Nb thin film surfaces

Ari D. Brown, Emily M. Barrentine, Samuel H. Moseley, Omid Noroozian, and Thomas Stevenson

***Abstract*—Polycrystalline superconducting Nb thin films are extensively used for submillimeter and millimeter transmission line applications and, less commonly, used in microwave kinetic inductance detector (MKID) applications. The microwave and *mm*-wave loss in these films is impacted, in part, by the presence of surface nitrides and oxides. In this study, glancing incidence x-ray diffraction was used to identify the presence of niobium nitride and niobium monoxide surface layers on Nb thin films which had been exposed to chemicals used in standard photolithographic processing. A method of mitigating the presence of ordered niobium monoxide surface layers is presented. Furthermore, we discuss the possibility of using glancing incidence x-ray diffraction as a non-destructive diagnostic tool for evaluating the quality of Nb thin films used in MKIDs and transmission lines. For a given fabrication process, we have both the x-ray diffraction data of the surface chemistry and a measure of the mm-wave and microwave loss, the latter being made in superconducting resonators.**

***Index Terms*—Superconducting integrated thin film circuits, superconducting photodetectors, dielectric films, dielectric losses.**

I. Introduction

A new class of superconducting spectrometers-on-a chip operating in the sub-mm to mm spectral bands, which includes μ-Spec [1], SuperSpec [2], and DESHIMA [3], are envisioned to become integral space-borne or balloon-borne instruments due to their compact size. The salient components that all three of these instruments have in common are superconducting microwave kinetic inductance detectors (MKIDs), superconducting transmission lines, and superconducting slot antennas. The MKIDs are read out at microwave frequency, and the incoming sub-mm and mm radiation is coupled via an antenna to planar superconducting transmission lines. In a similar manner, various MKID cameras have been realized for cosmic microwave background studies [4, 5]. Consequently, microwave and mm-wave loss in these components may have a deleterious impact on the optical efficiency, spectral bandwidth, and resolving power of these instruments.

One source of electromagnetic loss in superconducting components is the loss due to amorphous metal oxides and nitrides on the surface of superconducting films, which is correlated with two-level system (TLS) fluctuations [6]. Microwave [7] and millimeter [8] power is resonantly coupled to an ensemble of TLS, which contributes to loss in the material. Furthermore, suppression of the superconducting gap by the presence of lower T_c ordered oxides or nitrides can introduce unexpected loss at sub-*mm* frequency [9].

Various techniques may be used to identify the presence of surface nitrides and oxides, which include X-ray photoelectron spectroscopy [10], Rutherford backscattering spectroscopy [11], Auger electron spectroscopy, and glancing incidence x-ray diffraction [12]. Glancing or grazing incidence x-ray diffraction is a surface-sensitive technique, in which the sample is probed following the Bragg condition and Snell's law for total external reflection [13]. The latter case is applicable, because the refractive index of a dense material is less than unity at x-ray wavelength. Consequently, at angles of incidence below a critical angle ω_c the x-rays evanescently couple with the material. Thus, the x-ray penetration depth inside a material can vary over many orders of magnitude within a small angular range [14].

Here we use glancing incidence x-ray diffraction as a means to identify niobium oxides and nitride on the surface of niobium thin films that comprise the superconducting transmission lines and antenna on μ-Spec. We find that the presence of an ordered niobium monoxide phase is consistent with a high frequency cut-off observed in niobium sub-*mm* transmission lines of the spectrometer. Furthermore, we evaluate our fabrication process and find that the exposure of positive photoresist to niobium surfaces with a native oxide promotes the formation of ordered niobium monoxide, which appears to increase the intrinsic quality factor of microwave resonators. In addition, a simple means to prevent the formation of this ordered metal oxide layer is presented.

II. Detection of Surface Oxides on Nb Thin Film Surfaces

The motivation of searching for surface oxides on Nb thin films arises from an anomalous high frequency cut-off observed in a μ-Spec prototype [1]. μ-Spec operates by coupling sub-*mm* radiation (~400 GHz) to a slot antenna, and uses a phased superconducting transmission line network as a diffraction grating analog to separate different spectral components which are eventually detected by MKIDs [15].

Figure 1 shows the spectral response of the reference resonators on two μ-Spec devices, which were fabricated on two separate runs. The reference resonators bypass the spectrometer and are coupled to the slot antenna by 37 mm of

This work was supported by the National Aeronautics and Space Administration under NNH14ZDA001N-APRA.

The authors are with NASA Goddard Space Flight Center, Greenbelt, MD 20771 USA (e-mail: ari.d.brown@nasa.gov).

O. Noroozian is also with the Department of Astronomy at the University of Maryland, College Park, MD 20742 USA.

Nb microstrip line. The spectral response of the "new generation" device is characterized by a sharp high frequency cutoff at 450 GHz. In contrast, transmission down the microstrip line is attenuated much more slowly in the "old generation" device, and radiation ceases to propagate down the transmission line at a much higher frequency. It was expected that the high frequency cutoff would be approximated by the gap frequency of Nb~3.5-4 $k_B T_c/h$ ~ 630-750 GHz [16], because the microstrip transmission line is comprised of a Nb ground plane and Nb top layer separated by a 470 nm single crystal Si dielectric. Thus, it was suspected that one or both of the Nb layers in the new generation device either had bulk or surface contaminants, which might decrease T_c or increase the loss tangent, respectively, or high tensile stress, which has been shown to be responsible for an increase in the loss tangent of Nb thin films [17].

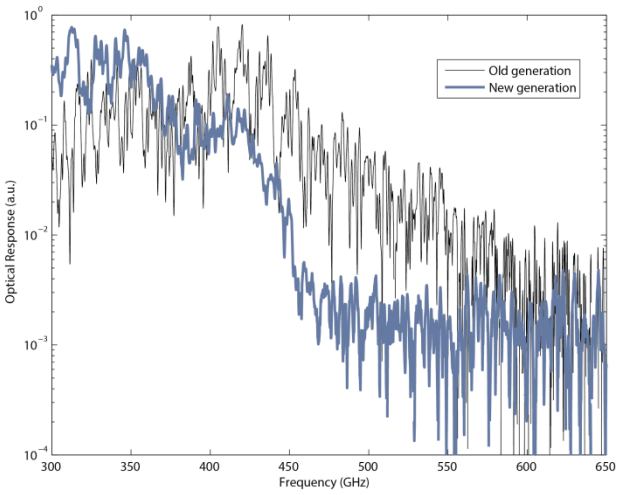

Fig. 1. Spectral response of the reference resonators on two μ-Spec devices. The reference resonators on both devices were coupled to a slot antenna via a Nb microstrip transmission line, which was comprised of a top Nb layer and Nb ground plane separated by a single crystal Si dielectric. The ground plane layers were deposited in a similar manner. Consequently, it was believed that the top Nb layer was responsible for the observed high-frequency cutoff.

Fabrication of the μ-Spec devices followed a process described in [18]. The Nb ground plane was DC magnetron sputter deposited (at 350 W and with 3.18 mT of Ar) and lifted off on a silicon-on-insulator (SOI) wafer, after which the Si device layer was bonded to a silicon handle wafer with Benzocyclobutene (BCB). A lift-off process was used to pattern the Nb, because an etch process would have resulted in removal of the Si dielectric by an uncontrolled amount and make characterization of the spectrometer response nearly impossible. The SOI handle wafer was then removed via mechanical lapping and deep reactive ion etching, and the buried oxide was etched with dilute HF. Aluminum or Mo_2N/Mo/Mo_2N MKIDs were deposited, patterned, and etched on the opposite side of the Si device layer (of the Nb ground plane) on the new and old generation devices, respectively, and the top Nb layers were lifted off. Palladium-gold resistive layers were lifted off and ground plane access regions were exposed with reactive ion etching of the Si device layer.

The last fabrication steps, which consisted of depositing an impedance matched coating on the wafer back side (for stray light mitigation) and dicing the individual μ-Spec dice, were the ones in which the processing for the new and old generation devices was substantially different. Fabrication of the old generation devices proceeded with: Coating of the top metal layers with a passivating polymer (Gen-Arc 365), wax bonding the wafer to a Pyrex wafer, lifting off a Bi impedance matched coating, dicing the parts, release in acetone, and ashing away the Gen-Arc. In contrast, the new generation devices were completed by coating the top metal layers with positive photoresist, depositing, patterning, and etching a Ti impedance matched coating, and dicing. Thus, we hypothesized that because the top Nb layers were subjected to different processing steps, either their surface chemistries or their film stress were different.

The initial means to determine whether there were surface impurities on the top Nb layer surface was performed with nulling ellipsometry measurements of the multimode region. The spectrometer multimode region was probed because it was comprised of the same Nb top layer, Si dielectric, and Nb ground plane as the Nb microstrip lines and it is much larger than the region illuminated by the ellipsometer. This latter point allowed one to probe a region on the μ-Spec surface that was homogeneous in the plane of the sample.

The first two rows in Table 1 describe the layer stack on top of the Nb surface of the completed MicroSpec dice. For all the devices, the range of Nb_2O_5 thickness values is similar to a value derived by d'Acapito *et al.*, [19], who used extended x-ray absorption fine structure spectra to measure the native oxide thickness of a Nb thin film which had been exposed to atmosphere for several weeks. The presence of an additional surface layer was also predicted. Unfortunately, we had no insight into the identity of this layer, because a B-Spline model used to fit the ellipsometric data yielded dielectric constants whose values were unphysical. By performing various etching tests on different new generation μ-Spec dice, it was inferred that the additional layer was positioned between the Nb and the Nb_2O_5.

TABLE I
ELLIPSOMETRIC PREDICTIONS OF SURFACE CONTAMINANTS ON TOP NB SURFACE

Surface Treatment	Nb_2O_5 Thickness [nm]	Additional Layer Thickness [nm]
None (old gen.)	3.1	1.5
None (new gen.)	2.6	1.7
36' O_2 ash, 200W, 175 mT	2.8	1.7
1' CF_4/O_2 etch, 100W, 85 mT	1.0	1.9
1' CHF_3/CF_4/Ar etch, 100W, 85 mT	0.7	2.0
20' Ar ion mill, 500V, 20 mA	0.0	1.2
30" dilute HF dip	0.4	1.7

Extracted values of surface layer thickness on top of the Nb multimode region on various μ-Spec parts. Four μ-Spec dice from the same "new generation" wafer were subjected to different surface treatments. An ellipsometric model predicted the presence of two distinct layers, which included Nb_2O_5 and an additional layer which had unphysical dielectric constants. This anomalous layer was the last to be removed upon exposure to various etchants. Consequently, it was believed that this layer was sandwiched between Nb_2O_5 and Nb.

Measurements of the Nb film stress were conducted via two methods. One method involved obtaining the global stress of the film on a witness wafer, which was coated with Nb at the same time as the μ-spec devices, using an FSM film stress measurement machine. The film stress measured with this technique ranged between -150 and +50 MPa.

The second method involved inferring the stress from glancing incidence x-ray diffraction data. Copper K_α x-rays were directed at a glancing angle ω which ranged between 0.1 and 8.0 degrees of the sample with an Equinox-100 (Inel) x-ray diffractometer in an asymmetric geometry. This angular range corresponded to an x-ray penetration depth ranging between 3.6 and 1105.4 nm in Nb. The Nb was found to be polycrystalline, with prominent (110), (200), and (211) diffraction peaks. Figure 2 shows that the lattice strain, $\varepsilon_{hkl}=(d_{hkl}-d_0)/d_0$, where d_0 is the bulk lattice parameter, of the Nb thin films can be described in terms of three regimes. Near the Nb/atmospheric interface, the Nb grains are highly strained, which suggests that a native oxide is responsible for the lattice deformation. For penetration depth slightly larger than the top Nb thickness (=270 nm), the (200)-oriented crystallites have a negative strain, which may suggest that the Si substrate is impacting the growth of the film. Finally for penetration depth > 500 nm, in which the ground plane is most likely being probed, the lattice strain is almost identical to that of the bulk value. The $\sin^2\Psi$ (where $\Psi=\theta-\omega$) method was used to estimate the stress [20] for a penetration depth much larger than the top Nb film thickness, which yielded stress values of ~190(110) and 670 (500) MPa in the [200] and [211] directions; in the [110] direction, the stress was found to be ~1.7 (1.0) GPa for penetration depth of 550-760 nm and -1.5 (-1.6) GPa for larger penetration depth for the new (old) generation device. Due the fact that there were two different Nb layers present it was difficult to ascertain which layer was stressed.

The stress values obtained using glancing incidence x-ray diffraction were similar for both the old and new generation μ-Spec parts. However, close examination of x-ray diffraction data taken after 20 hours of integration time and at a glancing incidence angle of 0.3 degrees, which corresponds to a penetration depth of 5 nm, illuminates a difference in surface composition.

Whereas x-ray diffraction on the multimode region on old generation devices (four devices) exhibited diffraction patterns corresponding to Nb, x-ray diffraction on new generation devices (four devices) exhibited patterns with additional diffraction peaks. Fig. 3 shows that the additional peaks are well described by NbN and NbO [21].

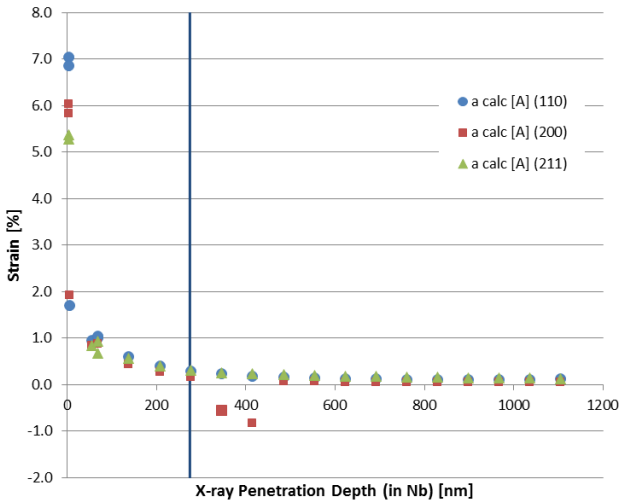

Fig. 2. The lattice strain of Nb in the multimode region on a new generation μ-Spec device. Near the Nb/atmospheric interface, the lattice strain is highly strained. The strain gradually vanishes near the Nb/Si interface (vertical line). A similar lattice strain versus x-ray penetration depth profile was also obtained on old generation μ-Spec devices.

We focused our attention on NbO, because its presence was observed on all the new generation devices while NbN was detected on only some of them. Niobium monoxide is a superconductor with T_c~1.38 K [22] and has been reported to be found, in a disordered combination with Nb_2O [23] or NbO_2 [24] between native Nb_2O_5 and Nb. Thus, a combination of these oxides might comprise the anomalous layer detected with ellipsometry in this study. The presence of a thick layer of NbO (>2 nm) between Nb_2O_5 and Nb has been correlated with a lower energy gap and increased losses in RF cavities due to the formation of strain-generated serration of Nb at the surface [9]. Consequently, the presence of a thick NbO layer might be undesirable in the transmission lines found on μ-Spec and, presumably, MKIDs.

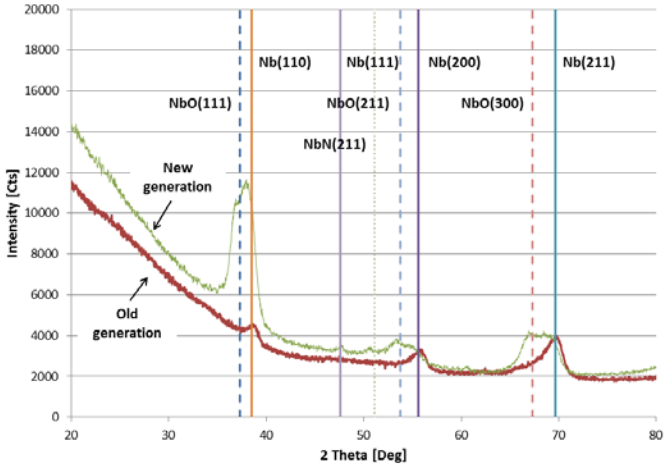

Fig. 3. Glancing incidence X-ray diffraction scans on the multimode region of a new and old generation μ-Spec device. The solid lines, dashed lines, and dotted line indicate the position of the Nb, NbO, and NbN diffraction peaks, respectively, which were observed only in the new generation devices. Whereas the labels for the Nb peaks are located to the right of the lines, the labels are located to the left of the lines for NbO and NbN. Note that in order to distinguish these peaks from the background, extremely long (10s of hours) integration times were used.

III. Source and Mitigation of Niobium Monoxide and Niobium Nitride on Nb Thin Film Surfaces

In order to further understand the processes responsible for the observation of pronounced NbO x-ray diffraction peaks on the new-generation μ-Spec devices, we performed a simple experiment on Nb-coated Si(001) wafers. As described above, one of the major differences between the old and new generation μ-Spec devices is that whereas the Nb surface of the old generation devices were exposed to Gen-Arc 365 during backside processing, the Nb on the new generation devices was exposed to positive photoresist (S-1827, Shipley). Thus, it was hypothesized that an Nb surface exposed to positive photoresist would have an ordered NbO surface layer, which would be seen in glancing incidence x-ray diffraction data.

The experiment consisted of spinning photoresist on a Nb-coated wafer, with, presumably, a native oxide layer on its surface, with the same spin speed and time used for coating the new generation μ-Spec wafers (3000 rpm, 30 sec). The resist was then soft baked on a vacuum hotplate for 1 min at 110 C in order to mimic the process used to prepare the wafer for dicing. Furthermore, the resist was hotplate baked for (1) an additional two minutes at 110 C in order to mimic the process used to protect the front side of the wafer in preparation for deposition of the backside Ti, and (2) an additional 30 minutes at 90 C in an oven in order to mimic the process used to pattern the Ti. Subsequently, the photoresist was stripped with organic solvents.

Figure 4 confirms our hypothesis, because well-defined diffraction peaks corresponding to NbO are clearly observed for the sample that had been coated with photoresist. In contrast, the diffraction pattern of a "control" sample, which consisted of a bare Nb film, exposed to atmosphere for two weeks, did not. Furthermore, when hexamethyldisilizane (HMDS) was used to passivate the Nb surface prior to coating it with photoresist, the clearly defined NbO diffraction peaks were not observed.

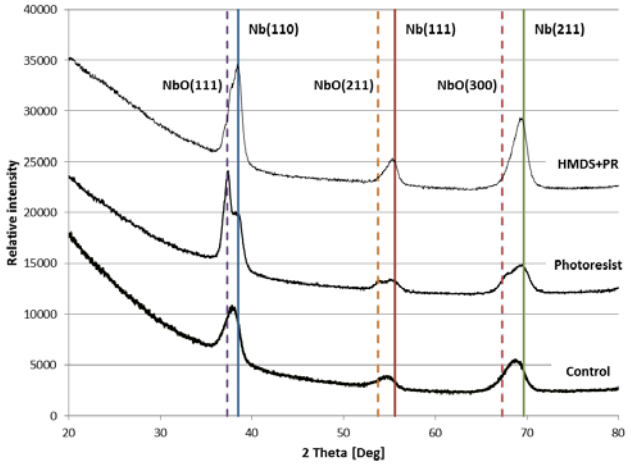

Fig. 4. Glancing incidence (angle = 0.3°) X-ray diffraction scans on unpatterned Nb thin films deposited on Si(001) substrates. The solid lines and dashed lines indicate the positions of the Nb and NbO diffraction peaks, respectively. The presence of positive photoresist (PR) on the Nb surface appears to promote the formation an ordered NbO layer.

At present, we are uncertain about the mechanism responsible for the formation of an ordered NbO layer on Nb surfaces exposed to positive photoresist. Perhaps the carbonyl group in the propylene glycol methyl ether acetate found in the photoresist is responsible for changing the oxidation state of the disordered layer located between Nb_2O_5 and Nb, and the HMDS serves as a barrier against such a reaction.

The impact of an ordered NbO layer on the microwave properties of Nb thin films was also studied. The resonators were fabricated by sputter depositing Nb on a fz Si(001) wafer (ρ>2000 Ωcm), passivating the Nb with HMDS, and patterning it with positive photoresist. The Nb was reactive ion etched with a CF_4/O_2 plasma, after which the resist was cleaned with an organic base (EKC-265). Then the wafer was cleaved in half and was prepared for dicing either by spinning on S-1811 photoresist and baking it using the protocol to generate the formation of an ordered NbO phase described earlier in this Section or by passivating the surface with HMDS and coating it with photoresist. At 165 mK, the value of the intrinsic quality factor ranged between 2 and $3x10^5$ and between 3 and $8x10^5$ (using -60 dBm of ~3.5 GHz radiation) for the passivated and unpassivated Nb, respectively. Furthermore, the latter devices had resonant frequency that was 10-40 MHz lower.

IV. Conclusions

The presence of an ordered NbO phase was detected using glancing incidence x-ray diffraction on Nb thin film surfaces exposed to positive photoresist. The formation of this phase appeared to be prevented by passivating the Nb surface with HMDS, and its presence might have impacted the millimeter and microwave properties of Nb. Further work, for instance, temperature sweeps of the microwave resonators performed in order to quantify the amount of TLS loss, is warranted to ascertain the impact of an ordered NbO phase on the surface of Nb thin film superconducting devices.

Acknowledgment

The authors would like to acknowledge Vilem Mikula for fabrication support.

References

[1] O. Noroozian, *et al.*, "μ-Spec: An Efficient Compact Integrated Spectrometer for Submillimeter Astrophysics," *26th Int. Symp. on Space Terahertz Tech.* Cambridge, MA, March 2015.

[2] S. Hailey-Dunsheath, *et al.*, "Optical Measurements of SuperSpec: A Millimeter-Wave On-Chip Spectrometer," *J. Low Temp. Phys.*, vol. 176, no. 5, Sept. 2014.

[3] A. Endo, *et al.*, "Development of DESHIMA: A Redshift Machine Based on a Superconducting On-Chip Fliterbank," *Proc. of SPIE*, vol. 8452, Jul. 2012.

[4] H. McCarrick, *et al.*, "Horn-coupled, commercially-fabricated aluminum lumped-element kinetic inductance detectors for millimeter wavelengths," *Rev. Sci. Instru.*, vol. 85, no. 12, Dec. 2014.

[5] M. Calvo, *et al.*, "The NIKA 2011 run: results and perspectives towards a permanent camera for the Pico Veleta observatory," *Proc. of SPIE*, vol. 8452, Jul. 2012.

[6] M. S. Khalil, "A Study of Two-Level System Defects in Dielectric Films Using Superconducting Resonators," Ph.D. dissertation, Dept. of Phys., U. of Maryland, College Park, MD, USA, 2013, unpublished.

[7] D. P. Pappas, *et al.*, "Two Level System Loss in Superconducting Microwave Resonators," *IEEE Trans. on Appl. Supercond.*, vol. 21, no. 3, June 2011.
[8] J. Gao, *et al.*, "Measurement of loss in superconducting microstrip at millimeter-wave frequencies," *Low Temp. Detectors LTD 13, Proc. of the 13th Intl. Workshop*, Eds. B. Cabrera, A. Miller, and B. Young, Melville, NY, USA: American Institute of Physics, 2009, pp. 164-167.
[9] J. Halbritter, "On the Oxidation and on the Superconductivity of Niobium," *Appl. Phys. A*, vol. 43, no. 1, May 1987.
[10] M. C. Biesinger *et al.*, "Resolving surface chemical states in XPS analysis of first row transition metal oxides and hydroxides: Cr, Mn, Fe, Co and Ni," *Appl. Surf. Sci.*, vol 257, no. 7, Jan. 2011.
[11] Y. Serruys, T. Sakout, and D. Gorse, "Anodic oxidation of titanium in 1M H_2SO_4 studied by Rutherford backscattering," *Surf. Sci.*, vol. 282, no. 3, Feb. 1993.
[12] F. J. Szalkowski and G. A. Somorjai, "Auger Electron Spectroscopy Investigations of the Surface Chemical Composition of Vanadium, the Vanadium Oxides, and Oxidized Vanadium: Chemical Shift and Peak Intensity Analysis," *The J. of Chem. Anal.*, vol 56, no. 12, June 1972.
[13] J. Szlachetko and Y. Kayser, "Techniques RXES, HR-XAS, HEROS, GIXRF, and GEXRF," in *High-Resolution XAS/XES: Analyzing Electronic Structures of Catalysts*, J. Sa, Ed. Boca Raton, FL, USA: CRC Press, 2015, pp. 80-84.
[14] S. Stepanov, "Grazing-Incidence X-ray Diffraction," *3rd Autumn School on X-ray Scattering from Surfaces and Thin Layers* (1997): 1-4.
[15] G. Cataldo, *et al.*, "Micro-Spec: an ultracompact, high-sensitivity spectrometer for far-infrared and submillimeter astronomy," *App. Opt.*, vol. 53, no. 6, Feb. 2014.
[16] A. V. Pronin, *et al.*, "Direct observation of the superconducting energy gap developing in the conductivity spectra of niobium," *Phys. Rev. B*, vol. 57, no. 22, June 1998.
[17] P. A. R. Ade, *et al.*, "Antenna-Coupled TES Bolometers Used in BICEP2, Keck Array, and SPIDER, *The Astrophys. Journal*, vol. 812, no. 2, Oct. 2012.
[18] A. Patel, *et al.*, "Fabrication of MKIDs for the MicroSpec Spectrometer," *IEEE Trans. Appl. Supercond.*, vol. 23, no. 3, June 2013.
[19] F. d'Acapito, *et al.*, "Temperature modification of the Nb oxidation at the Nb/Al interface studied by reflEXAFS," *Surf. Sci.*, vol. 468, no. 1-3, Nov. 2000.
[20] P. S. Prevey, "X-ray Diffraction Residual Stress Techniques," in Metals Handbook, 10, Metals Park, OH, USA: American Society for Metals, 1986, pp. 380-392.
[21] D. Bach, *et al.*, "EELS Investigation of Different Niobium Oxide Phases," *Microsc. Microanal.*, vol. 12, no. 5, Oct. 2006.
[22] J. K. Hulm, *et al.*, "Superconductivity in the TiO and NbO systems," *J. of Low Temp. Phys.*, vol. 7, no. 3, Nov. 1971.
[23] M. Grundner and J. Halbritter, "XPS and AES studies on oxide growth and oxide coatings on niobium," *J. Appl. Phys.*, vol. 51, no. 1, Jan. 1980.
[24] H. Hahn and H. J. Halama, "AES depth profile measurements of niobium for superconducting cavities," *J. Appl. Phys.*, vol. 47, no. 10, Oct. 1976.